Journal of Science and Technology

Numerical Solution of Mixed Convection Flow about a Sphere in a Porous Medium Saturated by a Nanofluid: Brinkman Model

Leony Tham[1], Roslinda Nazar[2,*]

[1] Faculty of Agro Industry and Natural Resources, Universiti Malaysia Kelantan, 16100 Pengkalan Chepa, Kota Bharu, Kelantan, Malaysia
[2]School of Mathematical Sciences, Faculty of Science & Technology, Universiti Kebangsaan Malaysia, 43600 UKM Bangi, Selangor, Malaysia

[*]*Corresponding e-mail: rmn@ukm.my*

Abstract

In the present study, the steady mixed convection boundary layer flow about a solid sphere with a constant surface temperature and embedded in a porous medium saturated by a nanofluid has been investigated via the Brinkman model for both the assisting and opposing flow cases. The resulting system of nonlinear boundary layer equations in the form of partial differential equations is solved numerically using an implicit finite-difference scheme known as the Keller-box method. Numerical results are obtained and discussed for the skin friction coefficient, local Nusselt number, local Sherwood number, velocity profiles, temperature profiles and nanoparticle volume fraction profiles. These results are presented for different values of the governing parameters, namely the mixed convection parameter and the Darcy-Brinkman parameter. It is found that the boundary layer separates from the sphere for some negative values of the mixed convection parameter (opposing flow). Increasing the mixed convection parameter delays the boundary layer separation and the separation can be completely suppressed for sufficiently large values of the mixed convection parameter.

Keywords: numerical solution; mixed convection flow; porous medium; nanofluid; brinkman model

1. INTRODUCTION

The “nanofluid” term was defined as the dilution of nanometer-sized particles (smaller than 100nm) in a fluid such as water, ethylene glycol and oil [1]. According to Khanafer et al., as the diluted nanoparticles size is extremely small, they can easily flow smoothly through the microchannels, and could improve the thermal conductivity and convective heat transfer coefficient compared to the base fluid only, and as such, nanofluids are widely used as coolants, lubricants and heat exchangers [2]. The utility of a particular nanofluid as a heat transfer medium can be established by modelling the convective transport in such nanofluid [3]. Meanwhile, Buongiorno and Hu considered a study on the convective transport in nanofluids and concluded that turbulence is not affected by the presence of the nanoparticles [4]. A comprehensive study on the nanofluids characteristics had also been well documented by Das et al. [5].

Convective heat transfer in porous medium is important in thermal engineering applications, such as geophysical thermal and insulation engineering, chemical catalytic reactors, ceramic processes, fiber and granular insulations and petroleum reservoirs. Many studies have been performed by Nield and Bejan [6] and Ingham and Pop [7], which focused on the free and mixed convection in porous media based on Darcy’s law and Forschheimer’s law, an extended Darcy’s law models. However, as Darcy’s law neglected the viscous force involved in convection heat transfer, and is only valid for slow viscous flow, that is with Reynolds number less than 1 cases, as such, Brinkman [8] introduced another Darcy’s extended law, the Brinkman model, which suggested that the momentum equation for a porous medium flow with a high permeability must be reduced to the viscous flow limit and advocated that classical frictional term to be included in the Darcy’s law. Further, the Brinkman model for the forced convection over an impermeable heated plate embedded in a porous medium was studied by Vafai and Tien [9] and they pointed that the viscous effect on the surface and the bulk viscous forces are equally important. Nazar et al. [10] considered the Brinkman model for the mixed convection boundary layer flow from a horizontal circular cylinder embedded in a fluid-saturated porous medium, and concluded that the results for the Brinkman model differed significantly than the results for Darcy’s law model, and the increased of the Darcy-Brinkman parameter led to the decreased of the surface heat transfer and the skin friction coefficient.

In this paper, the nanofluids equation model proposed by Buongiorno [11] and the transformations proposed by Nazar et al. [10] for the mixed convection boundary layer flow about a solid sphere immersed in a viscous (non-porous) and incompressible fluid are adopted to study the problem of mixed convection boundary layer flow about a solid sphere embedded in a porous medium saturated by a nanofluid using the Brinkman model.

2. ANALYSIS

Consider the steady mixed convection boundary layer flow about an impermeable solid sphere of radius a embedded in a porous medium filled with a nanofluid. It is assumed that the constant surface temperature of the sphere is T_w, while the constant ambient temperature is T_∞, where $T_w > T_\infty$ for a heated sphere (assisting flow) and $T_w < T_\infty$ for a cooled sphere (opposing flow). It is also assumed that the velocity of the external flow (inviscisd flow) or the local free stream velocity is $U_e(x)$, where x is the coordinate measured along the surface of the sphere starting from the lower stagnation point. It is assumed that the nanoparticles are suspended in the nanofluid using either surfactant or surface charge technology. We consider a porous medium whose porosity is denoted by φ and permeability by K. Under these assumptions along with the Oberbeck-Boussinesq approximation and the basic equations for the steady flow, we obtain the following boundary layer equations for the problem under consideration in dimensionless[12] form:

$$\frac{\partial (ru)}{\partial x} + \frac{\partial (rv)}{\partial y} = 0, \tag{1}$$

$$\frac{\partial u}{\partial y} = \Gamma \frac{\partial^3 u}{\partial y^3} + \left(\frac{\partial \theta}{\partial y} - Nr \frac{\partial \phi}{\partial y} \right) \lambda \sin x, \tag{2}$$

$$u \frac{\partial \theta}{\partial x} + v \frac{\partial \theta}{\partial y} = \frac{\partial^2 \theta}{\partial y^2} + Nb \frac{\partial \phi}{\partial y} \frac{\partial \theta}{\partial y} + Nt \left(\frac{\partial \theta}{\partial y} \right)^2, \tag{3}$$

$$Le \left(u \frac{\partial \phi}{\partial x} + v \frac{\partial \phi}{\partial y} \right) = \frac{\partial^2 \phi}{\partial y^2} + \frac{Nt}{Nb} \frac{\partial^2 \theta}{\partial y^2}, \tag{4}$$

with the boundary conditions

$$\begin{aligned} &v = 0, \quad u = 0, \quad \theta = 1, \quad \phi = 1 \quad \text{at} \quad y = 0, \\ &u \to u_e(x), \quad \theta \to 0, \quad \phi \to 0 \quad \text{as} \quad y \to \infty, \end{aligned} \tag{5}$$

where we assume that $u_e(x) = (3/2)\sin x$. Here θ and ϕ are the dimensionless temperature and nanoparticle volume fraction, respectively, $r(x)$ is the radial distance from the symmetrical axis to the surface of the sphere, Γ is the Darcy-Brinkman parameter, Le is the Lewis number, λ is the mixed convection parameter, Nr is the buoyancy ratio parameter, Nb is the Brownian motion parameter and Nt is the thermophoresis parameter, which are defined as

$$\begin{aligned} &\Gamma = \frac{\tilde{\mu}}{\mu_f} Da\, Pe, \quad Le = \frac{\alpha_m}{\varphi D_B}, \quad \lambda = \frac{Ra}{Pe}, \quad Nr = \frac{(\rho_p - \rho_{f\infty})(C_w - C_\infty)}{\rho_{f\infty} \beta (T_w - T_\infty)(1 - C_\infty)}, \\ &Nb = \frac{\varphi (\rho c)_p D_B (C_w - C_\infty)}{(\rho c)_f \alpha_m}, \quad Nt = \frac{\varphi (\rho c)_p D_T (T_w - T_\infty)}{(\rho c)_f \alpha_m T_\infty}, \end{aligned} \tag{6}$$

with $\varphi = \mu_f / \tilde{\mu}$, $Da = K/a^2$ and $Ra = (1\text{-}C_\infty)gK\beta(T_w\text{-}T_\infty)a/(v_f\,\alpha_m)$ being the porosity, the Darcy and the modified Rayleigh numbers for the porous medium, respectively, and v_f is the kinematic viscosity of the fluid. It is worth mentioning that $\lambda > 0$ is for the assisting flow ($T_w > T_\infty$), $\lambda < 0$ for the opposing flow ($T_w < T_\infty$) and $\lambda = 0$ corresponds to the forced convection flow.

Integrating equation (2) with the boundary conditions (5) at $y \to \infty$, introducing the stream function ψ, which is defined such that $u = \partial\psi / \partial y$ and $v = -\partial\psi / \partial x$, and introducing the variables $\psi = x\,r(x) f(x,y)$, $\theta = \theta(x,y)$, $\phi = \phi(x,y)$, we obtain

$$\frac{\partial f}{\partial y} = \Gamma \frac{\partial^3 f}{\partial y^3} + \left[\frac{3}{2} + (\theta - Nr\,\phi)\,\lambda\right]\frac{\sin x}{x}, \tag{7}$$

$$\frac{\partial^2 \theta}{\partial y^2} + f\frac{\partial \theta}{\partial y} + Nb\frac{\partial \phi}{\partial y}\frac{\partial \theta}{\partial y} + Nt\left(\frac{\partial \theta}{\partial y}\right)^2 = x\left(\frac{\partial f}{\partial y}\frac{\partial \theta}{\partial x} - \frac{\partial f}{\partial x}\frac{\partial \theta}{\partial y}\right), \tag{8}$$

$$\frac{\partial^2 \phi}{\partial y^2} + Le\,f\frac{\partial \phi}{\partial y} + \frac{Nt}{Nb}\frac{\partial^2 \theta}{\partial y^2} = Le\,x\left(\frac{\partial f}{\partial y}\frac{\partial \phi}{\partial x} - \frac{\partial f}{\partial x}\frac{\partial \phi}{\partial y}\right), \tag{9}$$

with the boundary conditions

$$\begin{aligned} &f = 0, \quad \partial f / \partial y = 0, \quad \theta = 1, \quad \phi = 1 \quad \text{at} \quad y = 0, \\ &\partial f / \partial y \to (3/2)\sin x / x, \quad \theta \to 0, \quad \phi \to 0 \quad \text{as} \quad y \to \infty. \end{aligned} \tag{10}$$

It is worth mentioning that when Nr, Nb and Nt are all zero, equations (8) and (9) involve just two dependent variables, namely f and θ, and the boundary-value problem for these two variables reduces to the corresponding problem of the mixed convection boundary layer flow about a sphere embedded in a fluid-saturated porous medium using the Darcy-Brinkman model (The boundary value problem for ϕ then becomes ill-posed and is of no physical significance).

Quantities of practical interest are the skin friction coefficient C_f, the local Nusselt number Nu and the local Sherwood number Sh, which are defined as

$$\mathrm{C}_f = \frac{\tau_w}{\rho U_\infty^2}, \quad Nu = \frac{a\,q_w}{k_m(T_w - T_\infty)}, \quad Sh = \frac{a\,q_m}{D_B(C_w - C_\infty)}, \tag{11}$$

where τ_w, q_w, and q_m are the wall shear stress, the wall heat flux and the mass heat flux from the surface of the sphere, respectively, which are given by

$$\tau_w = \mu_f\left(\frac{\partial \bar{u}}{\partial \bar{y}}\right)_{\bar{y}=0}, \quad q_w = -k_m\left(\frac{\partial T}{\partial \bar{y}}\right)_{\bar{y}=0}, \quad q_m = -D_B\left(\frac{\partial C}{\partial \bar{y}}\right)_{\bar{y}=0}, \tag{12}$$

where k_m is the effective thermal conductivity of the porous medium. Substituting variables of boundary layer approximations and stream functions into (11) and (12), we obtain

$$(\mathrm{Pr}\, Pe^{1/2})\, C_f = x\frac{\partial^2 f}{\partial y^2}(x,0), \quad Pe^{-1/2}\, Nu = -\frac{\partial \theta}{\partial y}(x,0), \quad Pe^{-1/2}\, Sh = -\frac{\partial \phi}{\partial y}(x,0), \tag{13}$$

where $\mathrm{Pr} = \nu_f / \alpha_m$ is the Prandtl number for the porous medium.

3. RESULTS AND DISCUSSION

Equations (7) to (9) subject to the boundary conditions (10) have been solved numerically for different values of the parameters Γ, Le and λ, and at some streamwise positions x, using an efficient implicit finite-difference scheme known as the Keller-box method along with the Newton's linearization technique as described by Cebeci and Bradshaw [13] for both the assisting ($\lambda > 0$) and opposing ($\lambda < 0$) flow cases. The skin friction coefficient $(\mathrm{Pr}\, Pe^{1/2})\, C_f$, the local Nusselt number $Pe^{-1/2} Nu$, the local Sherwood number $Pe^{-1/2} Sh$, the velocity profiles $f'(y)$, the temperature profiles $\theta(y)$, and the nanoparticles volume fraction profiles $\phi(y)$, have been obtained for the following range of parameters: mixed convection parameter, $\lambda = 1$ (assisting flow), Γ Daryc-Brinkman parameter, Lewis number, $Le = 2$, 6 and 10, Brownian number, $Nb = 0.5$, buoyancy ratio parameter, $Nr = 0.5$, and thermophoresis parameter, $Nt = 0.5$, at different positions x. It seems that the values of the parameters considered usually exist in geophysical and engineering applications [14].

Some values of the skin friction coefficient, $(\mathrm{Pr}\, Pe^{1/2})\, C_f$, the local Nusselt number, $Pe^{-1/2} Nu$, the local Sherwood number $Pe^{-1/2} Sh$, are given in Tables 1 to 3 for some values of $Le = 2$, $\Gamma = 0.1$, $Nb = 0.5$, $Nr = 0.5$, $Nt = 0.5$ and various values of λ. These tables show that the boundary layer separates from the sphere for some values of $\lambda < 0$ (opposing flow). Increasing λ delays separation and the separation can be completely suppressed in the range $0 \le x < 120^{\circ}$ for sufficiently large values of λ. A value of $\lambda = \lambda_0 (< 0)$ is found below which the boundary layer solution is not possible. The actual value of $\lambda = \lambda_s (< 0)$ which first gives no separation is difficult to determine exactly as it has to be found by successive integration of the equations. However, the numerical solutions indicate that the value of λ_s which first gives no separation lies between -2.99 and -3.

Our objective is to observe the influence of the parameters Γ and Le on the heat, mass and fluid flow characteristics, and thus we will present the results in figure forms for the above parameters effect. Figures 1 and 2 show the variations of the skin friction coefficient, $(\mathrm{Pr}\, Pe^{1/2})\, C_f$ with the parameters Γ and Le, respectively.

The skin friction coefficient increases with the increase in the parameters Le, while decreases with increasing Γ. Figures 3 and 4 show the variations of the local Nusselt number $Pe^{-1/2}Nu$ with the parameters Γ and Le, respectively. The local Nusselt number decreases with the increase of parameters Γ and Le, which corresponds to an increase in the thermal boundary layer thickness. Figures 5 and 6 show the variations of the local Sherwood number $Pe^{-1/2}Sh$ with the parameters Γ and Le, respectively. The pattern of the effects is similar to the case of skin friction coefficient, that is, the local Sherwood number increases with the increase in the parameters Le, while decreases with increase of Γ.

The samples of velocity, temperature and the nanoparticle volume fraction profiles are given in Figures 7 and 8. In Figure 7, it is observed that the thicknesses of the thermal and the mass fraction boundary layers decrease with increasing values of Le. The increasing of Lewis number tends to increase the buoyancy-induced flow along the surface at the expense of the reduced concentration and its boundary layer thickness. From the observation made on Figures 7 and 8, the profiles satisfy the far field boundary conditions (10) asymptotically, which support the numerical results obtained.

Table 1: Values of skin friction coefficient $(\mathrm{Pr}\, Pe^{1/2})C_f$ for $\Gamma = 0.1$, $Le = 2$, $Nb = 0.5$, $Nr = 0.5$, $Nt = 0.5$ and various values of λ.

x	λ										
	- 3.04	- 3.01	- 3.0	- 2.99	- 2.0	-1.0	0	1.0	2.0	5.0	10.0
0^o	0.0000	0.0000	0.0000	0.0000	0.0000	0.0000	0.0000	0.0000	0.0000	0.0000	0.0000
10^o	0.0023	0.0083	0.0113	0.0143	0.2967	0.5653	0.8233	1.0733	1.3168	2.0184	3.1189
20^o	0.0036	0.0154	0.0213	0.0272	0.5830	1.1122	1.6207	2.1136	2.5940	3.9779	6.1497
30^o	0.0030	0.0202	0.0288	0.0374	0.8493	1.6236	2.3680	3.0901	3.7941	5.8232	9.0094
40^o	0.0001	0.0221	0.0331	0.0441	1.0868	2.0833	3.0426	3.9737	4.8819	7.5016	11.6187
50^o		0.0208	0.0338	0.0469	1.2879	2.4773	3.6239	4.7379	5.8253	8.9647	13.9044
60^o		0.0167	0.0313	0.0460	1.4463	2.7934	4.0944	5.3598	6.5961	10.1696	15.8006
70^o		0.0104	0.0262	0.0419	1.5577	3.0222	4.4397	5.8204	7.1708	11.0797	17.2505
80^o		0.0030	0.0194	0.0358	1.6192	3.1571	4.6494	6.1054	7.5314	11.6661	18.2080
90^o			0.0123	0.0287	1.6301	3.1945	4.7171	6.2057	7.6657	11.9081	18.6382
100^o			0.0058	0.0218	1.5910	3.1341	4.6408	6.1174	7.5681	11.7940	18.5192
110^o			0.0007	0.0159	1.5045	2.9784	4.4230	5.8423	7.2395	11.3214	17.8422
120^o				0.0108	1.3743	2.7331	4.0701	5.3876	6.6875	10.4978	16.6121

Table 2: Values of local Nusselt number $Pe^{-1/2}Nu$ for $\Gamma = 0.1$, $Le = 2$, $Nb = 0.5$, $Nr = 0.5$, $Nt = 0.5$ and various values of λ.

x	λ										
	- 3.04	- 3.01	- 3.0	- 2.99	- 2.0	-1.0	0	1.0	2.0	5.0	10.0
0^o	0.2288	0.2325	0.2343	0.2360	0.3483	0.4160	0.5487	0.5091	0.5450	0.6312	0.7361
10^o	0.2276	0.2313	0.2331	0.2349	0.3470	0.4147	0.4774	0.5076	0.5435	0.6295	0.7342
20^o	0.2243	0.2280	0.2298	0.2315	0.3435	0.4108	0.4689	0.5032	0.5390	0.6246	0.7289
30^o	0.2189	0.2225	0.2243	0.2261	0.3376	0.4044	0.4604	0.4962	0.5316	0.6166	0.7200
40^o	0.2115	0.2152	0.2170	0.2187	0.3294	0.3956	0.4500	0.4863	0.5214	0.6054	0.7077
50^o		0.2060	0.2078	0.2095	0.3191	0.3843	0.4374	0.4737	0.5082	0.5910	0.6919
60^o		0.1952	0.1970	0.1987	0.3065	0.3705	0.4223	0.4582	0.4922	0.5734	0.6725
70^o		0.1831	0.1849	0.1865	0.2919	0.3544	0.4047	0.4400	0.4732	0.5526	0.6494
80^o		0.1703	0.1719	0.1735	0.2753	0.3359	0.3846	0.4190	0.4512	0.5284	0.6226
90^o			0.1588	0.1601	0.2567	0.3150	0.3619	0.3952	0.4263	0.5009	0.5920
100^o			0.1465	0.1475	0.2362	0.2918	0.3366	0.3685	0.3982	0.4698	0.5573
110^o			0.1364	0.1369	0.2141	0.2664	0.3087	0.3388	0.3670	0.4350	0.5184
120^o				0.1292	0.1902	0.2386	0.2780	0.3061	0.3325	0.3963	0.4747

Table 3: Values of local Sherwood number $Pe^{-1/2}Sh$ for $\Gamma = 0.1$, $Le = 2$, $Nb = 0.5$, $Nr = 0.5$, $Nt = 0.5$ and various values of λ.

x	λ										
	- 3.04	- 3.01	- 3.0	- 2.99	- 2.0	-1.0	0	1.0	2.0	5.0	10.0
0^o	0.5051	0.5130	0.5168	0.5206	0.7622	0.9069	1.0404	1.1052	1.1819	1.3659	1.5905
10^o	0.5024	0.5103	0.5142	0.5180	0.7594	0.9039	1.0101	1.1019	1.1784	1.3621	1.5864
20^o	0.4950	0.5030	0.5069	0.5107	0.7516	0.8955	1.0007	1.0926	1.1688	1.3516	1.5748
30^o	0.4831	0.4910	0.4949	0.4988	0.7388	0.8817	0.9865	1.0773	1.1529	1.3343	1.5557
40^o	0.4668	0.4748	0.4787	0.4825	0.7211	0.8625	0.9665	1.0560	1.1307	1.3101	1.5291
50^o		0.4545	0.4584	0.4623	0.6986	0.8380	0.9407	1.0287	1.1024	1.2791	1.4949
60^o		0.4308	0.4347	0.4385	0.6714	0.8083	0.9092	0.9954	1.0677	1.2412	1.4531
70^o		0.4043	0.4081	0.4118	0.6397	0.7734	0.8720	0.9562	1.0268	1.1963	1.4034
80^o		0.3762	0.3797	0.3831	0.6036	0.7334	0.8292	0.9109	0.9795	1.1443	1.3458
90^o			0.3510	0.3539	0.5633	0.6884	0.7808	0.8596	0.9258	1.0850	1.2799
100^o			0.3244	0.3265	0.5190	0.6384	0.7267	0.8021	0.8655	1.0182	1.2054
110^o			0.3029	0.3038	0.4709	0.5834	0.6668	0.7383	0.7985	0.9436	1.1218
120^o				0.2879	0.4193	0.5234	0.6011	0.6679	0.7243	0.8604	1.0282

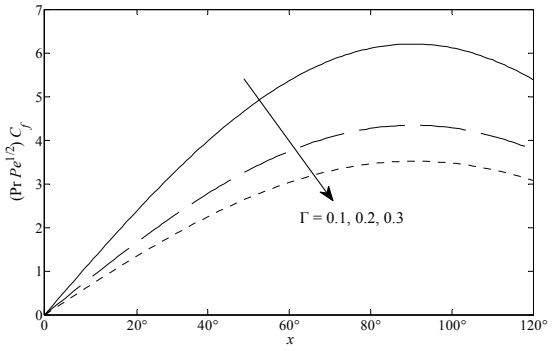

Figure 1: Variation of the skin friction coefficient $(\Pr Pe^{1/2})C_f$ with x for $\Gamma = 0.1,\ 0.2,\ 0.3$, $Le = 2$, $Nb = 0.5$, $Nr = 0.5$, $Nt = 0.5$ and $\lambda = 1$

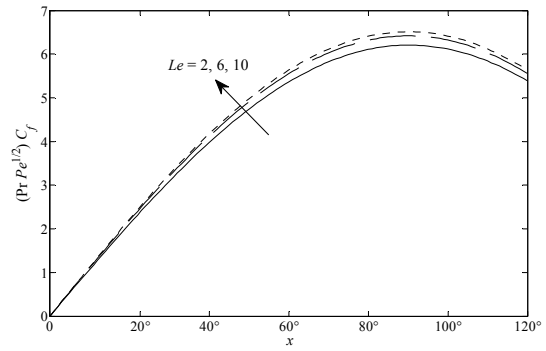

Figure 2: Variation of the skin friction coefficient $(\Pr Pe^{1/2})C_f$ with x for $\Gamma = 0.1$, $Le = 2,\ 6,\ 10$, $Nb = 0.5$, $Nr = 0.5$, $Nt = 0.5$ and $\lambda = 1$

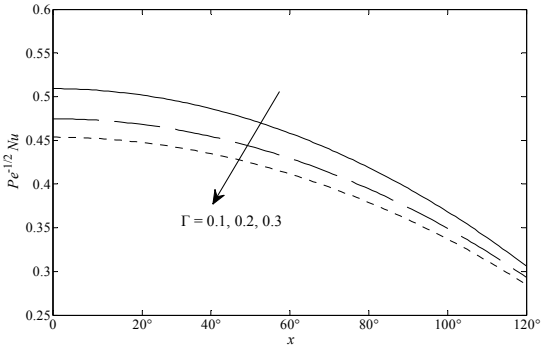

Figure 3: Variation of the local Nusselt number $Pe^{-1/2}Nu$ with x for $\Gamma = 0.1,\ 0.2,\ 0.3$, $Le = 2$, $Nb = 0.5$, $Nr = 0.5$, $Nt = 0.5$ and $\lambda = 1$

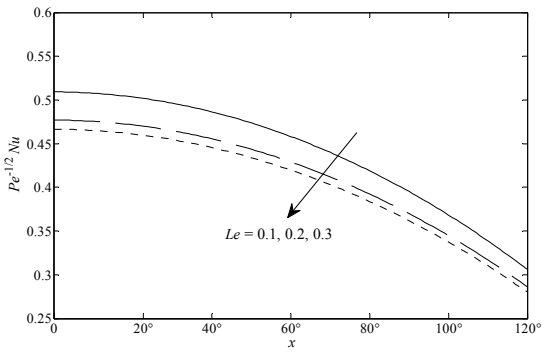

Figure 4: Variation of the local Nusselt number $Pe^{-1/2}Nu$ with x for $\Gamma = 0.1$, $Le = 2,\ 6,\ 10$, $Nb = 0.5$, $Nr = 0.5$, $Nt = 0.5$ and $\lambda = 1$

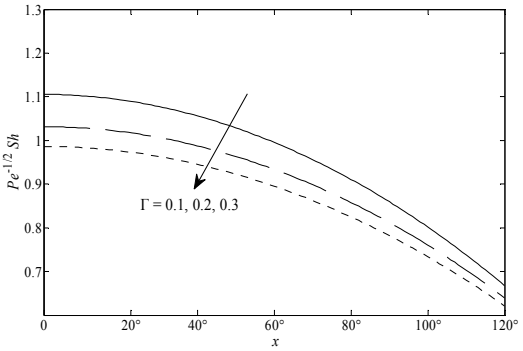

Figure 5: Variation of the local Sherwood number $Pe^{-1/2}Sh$ with x for $\Gamma = 0.1,\ 0.2,\ 0.3$, $Le = 2$, $Nb = 0.5$, $Nr = 0.5$, $Nt = 0.5$ and $\lambda = 1$

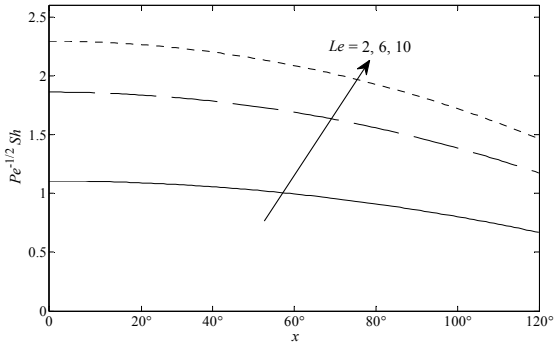

Figure 6: Variation of the local Sherwood number $Pe^{-1/2}Sh$ with x for $\Gamma = 0.1$, $Le = 2,\ 6,\ 10$, $Nb = 0.5$, $Nr = 0.5$, $Nt = 0.5$ and $\lambda = 1$

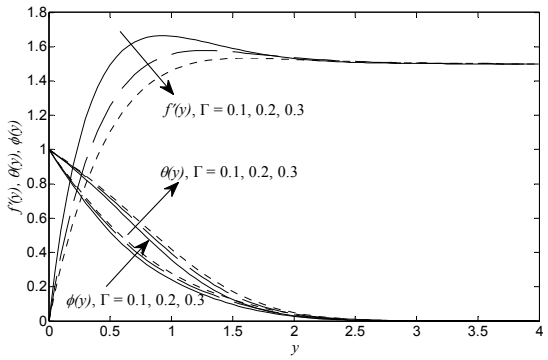

Figure 7: Variation of the velocity profiles $f'(y)$, temperature profiles $\theta(y)$ and the nanoparticles volume fraction profiles $\phi(y)$ at $x = 0$ for $\Gamma = 0.1,\ 0.2,\ 0.3$, $Le = 2$, $Nb = 0.5$, $Nr = 0.5$, $Nt = 0.5$ and $\lambda = 1$

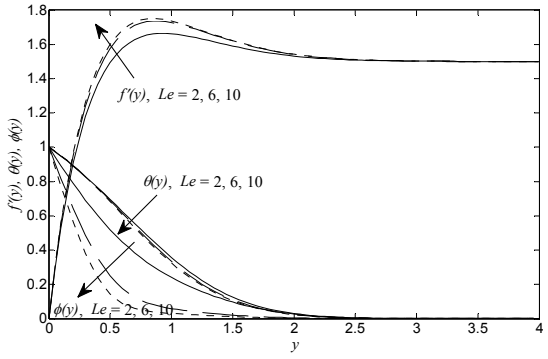

Figure 8: Variation of the velocity profiles $f'(y)$, temperature profiles $\theta(y)$ and the nanoparticles volume fraction profiles $\phi(y)$ at $x = 0$ for $\Gamma = 0.1$, $Le = 2,\ 6,\ 10$, $Nb = 0.5$, $Nr = 0.5$, $Nt = 0.5$ and $\lambda = 1$

4. CONCLUSIONS

In this paper, we have studied the problem of steady mixed convection boundary layer flow about a solid sphere with a constant surface temperature and embedded in a porous medium saturated by a nanofluid with Buongiorno-Brinkman model. From this study, we could draw the following conclusions for the assisting flow case: the skin friction coefficient, $(\Pr Pe^{1/2})C_f$ and the local Sherwood number $Pe^{-1/2}Sh$ increased when the value of the Lewis number Le, Brownian number Nb and thermophoresis parameter Nt increased, while opposite effect observed for Darcy-Brinkman parameter Γ and buoyancy ratio parameter Nr; the local Nusselt number, $Pe^{-1/2}Nu$ decreased when the value of the Darcy-Brinkman parameter Γ, Lewis number Le, buoyancy ratio parameter Nr, and thermophoresis parameter Nt increased, while opposite effect observed for Brownian number Nb.

Acknowledgment

The authors would like to acknowledge the financial support received in the form of fundamental research grant scheme (FRGS) from the Ministry of Higher Education, Malaysia.

REFERENCES

[1] Choi, S. (1995). "Enhancing thermal conductivity of fluids with nanoparticles" in: The Proceedings of the 1995 ASME International Mechanical Engineering Congress and Exposition, San Francisco, USA, ASME, FED 231/MD., 99-105.

[2] Khanafer, K -., Vafai, K. & Lightstone, M. (2003). "Buoyancy-driven heat transfer enhancement in a two dimensional enclosure utilizing nanofluids" in Int. J. Heat Mass Trasfer, Vol. 46 pp. 3639-3653..

[3] Kumar, S., Prasad, S.K. & Banerjee, J. (2010). "Analysis of flow and thermal field in nanofluid using a single phase thermal dispersion model" in Appl. Math. Modelling, Vol. 34 pp. 573-592.Brinkman, H. C. (1947). "A calculation of the viscous force exerted by a flowing fluid on a dense swarm of particles" in Appl. Sci. Res., Vol. 1 pp. 27–34.

[4] Buongiorno, J. & Hu, W. (2005). "Nanofluid coolants for advanced nuclear power plants" Paper no. 5705, in: Proceedings of ICAPP '05, Seoul.

[5] Das, S.K., Choi, S.U.S. Yu, W. & Pradet, T. (2007). Nanofluids: Science and Technology. Wiley, New Jersey.

[6] Nield, D.A. & Bejan, A. (1999). Convection in Porous Media, second ed.. Springer, New York.

[7] Ingham, D.B. & Pop, I. (1998). Transport Phenomena in Porous Media. Pergamon, Oxford

[8] Brinkman, H. C. (1947). "A calculation of the viscous force exerted by a flowing fluid on a dense swarm of particles" in Appl. Sci. Res., Vol. 1 pp. 27–34.

[9] Vafai, K. & Tien, C.L. (1981). "Boundary and inertia effects on flow and heat transfer in porous media" in Int. J. Heat Mass Transfer, Vol. 24 pp. 195-203.

[10] Nazar, R., Amin, N. & Pop, I. (2002). "On the mixed convection boundary-layer flow about a solid sphere with constant surface temperature" in Arab. J. Sci. & Eng., Vol. 27 pp. 117-135.

[11] Buongiorno, J. (2006). "Convective transport in nanofluids" in ASME J. Heat Transfer, Vol. 128 pp. 240-250.

[12] Kuznetsov, A.V. & Nield, D.A. (2009). "Thermal instability in a porous medium layer saturated by a nanofluid: Brinkman model" in Trans. Porous Media, Vol. 81 pp. 409-422

[13] Cebeci, T. & Bradshaw, P. (1984) Physical and Computational Aspects of Convective Heat Transfer. Springer, New York.

[14] Nield, D.A. & Kuznetsov, A.V. (2009). "The Cheng–Minkowycz problem for natural convective boundary-layer flow in a porous medium saturated by a nanofluid" in Int. J. Heat Mass Transfer, Vol. 52 pp. 5792–5795 at Mass Transfer, Vol. 24 pp. 195-203.